Assessment of the developmental toxicity of nanoparticles in an ex vivo 3D model, the murine limb bud culture system

Emilia Bigaeva, France-Hélène Paradis, Alexandre Moquin, Barbara F. Hales & Dusica Maysinger

Nanotoxicology

informa
healthcare

ORIGINAL ARTICLE

Assessment of the developmental toxicity of nanoparticles in an *ex vivo* 3D model, the murine limb bud culture system

Emilia Bigaeva[1,2]*, France-Hélène Paradis[1]*, Alexandre Moquin[1], Barbara F. Hales[1], and Dusica Maysinger[1]

[1]Department of Pharmacology and Therapeutics, McGill University, Montreal, Quebec, Canada and [2]Department of Pharmacokinetics, Toxicology and Targeting, Groningen Research Institute of Pharmacy, University of Groningen, Groningen, The Netherlands

Abstract

The rapid growth of nanotechnological products for biomedical applications has exacerbated the need for suitable biological tests to evaluate the potential toxic effects of nanomaterials. The possible consequences of exposure during embryo and fetal development are of particular concern. The limb bud culture is an *ex vivo* 3D model in which growth, cell differentiation, and tissue organization occur and both molecular and functional endpoints can be quantitatively assessed. We employed this model to assess biochemical and morphological changes induced during organogenesis by two classes of nanostructured materials: quantum dot nanocrystals and organic polyglycerol sulfate dendrimers (dPGS). We show that quantum dots carrying mercaptopropionic acid (QD-MPA) on the surface, commonly used in biological studies, inhibit the development of limb buds from CD1 wildtype and *Col2a1*; *Col10a1*; *Col1a1* triple transgenic fluorescent reporter mice, as revealed by changes in several morphological and biochemical markers. QD-MPA interfere with chondrogenesis and osteogenesis and disrupt the expression of COL10A1 and COL1A1, key markers of differentiation. In contrast, equivalent (3–100 nM) concentrations of dPGS do not adversely affect limb development. Neither QD-MPA nor dPGS-Cy5 alters the expression of several markers of cell proliferation or apoptosis. Collectively, these results suggest that murine limb buds in culture constitute a convenient, inexpensive and reliable developmental model for the assessment of the nanotoxicological effects of nanocrystals and polymers. In these 3D cultures, any effect that is observed can be directly ascribed to the nanostructures *per se* or a degradation component released from the complex nanostructure.

Introduction

As exposure to nanomaterials during pregnancy increases, so does the risk of adverse effects during development. Some of the various *in vitro* assays and *in vivo* studies that have been done to examine commercial products containing engineered nanomaterials (Hong et al., 2014; Magdolenova et al., 2014; Oberdörster, 2010; Ucciferri et al., 2014) have shown nanomaterial transfer across the placenta (Chan & Shiao, 2008; Chu et al., 2010; King Heiden et al., 2007; Menjoge et al., 2011; Wick et al., 2010). In animal models, fetal exposure to nanoparticles is influenced by the stage of pregnancy in addition to the nanomaterial size and surface composition (Yang et al., 2012). However, data on the embryotoxicity of various types of nanomaterials are still lacking. Indeed, few nanomaterials have been subjected to reproductive or developmental toxicity studies conducted in accordance with the Organization for Economic Co-operation and Development

(OECD) test guidelines (reviewed in Ema et al., 2010; Sun et al., 2013). Guideline-based tests assess risks to developing human embryos/fetuses by exposing pregnant animals (primarily rodents and rabbits) throughout organogenesis; these studies are lengthy and expensive so they are often not undertaken until a late stage in the development of products designed for human use. Materials that are not designated for human use may not be tested at all.

The availability and validation of *in vitro*/*ex vivo* model systems would permit the rapid, reliable and economical screening of nanostructured materials for their potential developmental toxicity. One example of such a model system is the murine limb bud in culture. Limbs cultured in a chemically defined medium undergo extensive differentiation in a three-dimensional manner, similar to that occurring *in vivo* (Paradis et al., 2012). The limb cartilaginous anlagen develop through a process that involves regulation of the expression of key markers of chondrogenesis and osteogenesis, including COL2A1, COL10A1 and COL1A1. Limb buds in culture have been used to study the molecular mechanisms of teratogen-induced disruptions of normal development for more than 30 years (Friedman, 1987; Kochhar, 1983; Neubert & Barrach, 1977). Today, limb bud cultures are used to elucidate the mechanisms by which chemicals interfere with critical signaling pathways in organogenesis (Paradis et al., 2012).

*These authors contributed equally to this work.

Correspondence: Dusica Maysinger, Department of Pharmacology and Therapeutics, McGill University, 3655 Promenade Sir-William-Osler, McIntyre Medical Sciences Building, Montreal, QC H3G 1Y6, Canada. Tel: +1514398 1264. Fax: +1514398 6690. E-mail: dusica.maysinger@mcgill.ca

Among the many different nanotechnological products, quantum dots (QDs) attract attention because of their unique physicochemical and optical properties (Alivisatos et al., 2005; Gao et al., 2005; Pelaz et al., 2012). These properties include high fluorescent quantum yield, size-tunable emission and a broad absorption spectrum, ranging from ultraviolet to infrared wavelengths. Moreover, the exceptional photostability of QDs makes them more suitable, compared with organic fluorescent dyes, for biomedical labeling and imaging applications, particularly for long term, multiplexed detection and *in vivo* imaging (Chatterjee et al., 2014; Jaiswal et al., 2003; Michalet et al., 2005; Wang & Chen, 2011). QDs are composed of a semiconductor core (e.g. CdSe and CdTe), and are often capped with a shell (e.g. ZnS) to improve core stability. Several mechanisms of QD toxicity have been proposed based on numerous studies *in vitro* using cells in monolayers. QD-induced cell death involves the formation of reactive oxygen species (ROS) due to the degradation of the QD core and the release of free cadmium ions (Derfus et al., 2003; Winnik & Maysinger, 2012), followed by oxidative stress and inflammation (Lovrić et al., 2005; Manke et al., 2013). In addition, exposure to QDs may cause cell growth inhibition and lipid peroxidation (Choi et al., 2007) as well as epigenetic and genetic changes (Choi et al., 2008; Stoccoro et al., 2013). The extent of QD toxicity depends on core composition, size, shape, surface coating, ligand arrangement and charge (Hoshino et al., 2004; Jiang et al., 2008; Kauffer et al., 2014; Verma & Stellacci, 2010). In the present studies, we employed QDs as potentially toxic nanocrystals which may exert toxic effects due to their poor stability and the leakage of cadmium or their inherent nanocrystal properties. In parallel, we tested organic dendrimers that are generally thought to be non-toxic (Dernedde et al., 2010; Kannan et al., 2014; Khandare et al., 2012), although early poly(ethylene imine) dendrimers were of limited use for clinical purposes due to their toxicity (Beyerle et al., 2010). Several dendrimer-derived products are already on the market as *in vitro* transfection agents (PolyFect® and Superfect®, Qiagen, Toronto, Canada). Dendrimer toxicity depends on size, charge, functional groups and dendron unit structures (Duncan & Izzo, 2005). Polyamidoamine, poly-L-lysine and poly(propylene imine) dendrimers exert significant *in vitro* and *in vivo* cytotoxicity due to their positively charged surfaces, mediating binding to negatively charged cell membranes (Agashe et al., 2006; Albertazzi et al., 2012; Kolhatkar et al., 2007; Ziemba et al., 2011). In contrast, compounds based on dendritic polyglycerols (dPG) show high biocompatibility, comparable to that of poly(ethylene glycol), one of the most well-studied biocompatible polymers (Calderón et al., 2010; Frey & Haag, 2002; Kainthan et al., 2006).

The aim of our study was to determine the suitability of the limb bud model to investigate the effects of two representative nanomaterials (nanocrystals and dendritic structure) during organogenesis. Two classes of nanostructured materials were studied: CdSe/CdZnS QDs with mercaptopropionic acid on the surface (QD-MPA) and Cy5-labeled dendritic polyglycerol sulfate (dPGS-Cy5). Valproic acid (VPA), a well-established teratogen (Ornoy, 2006), was used for comparison with the morphological changes following QD-MPA and dPGS-Cy5 exposures. VPA causes a significant concentration-dependent increase in limb abnormalities due to deregulation of the expression of target genes directly involved in chondrogenesis and osteogenesis in the developing limb (Paradis & Hales, 2013). We report that QD-MPA exposure at high concentrations (100 nM) inhibits the growth and differentiation of the cartilaginous anlagen in developing mouse limbs; interestingly, these effects were not accompanied by significant changes in the expression of markers of cell proliferation or apoptosis. In contrast, exposure to equimolar concentrations of dPGS-Cy5 has no adverse effects.

Methods

Nanoparticle preparation and characterization

MPA-coated CdSe/CdZnS core/shell QDs were synthesized, purified and characterized as briefly described in our previous study (Al-Hajaj et al., 2011); details are provided in the supplemental materials. The optical properties were determined by UV–Vis absorption spectrometry and spectrofluorometry. Transmission electron microscopy (TEM) was used to confirm the sizes of the electron dense nanocrystals. The hydrodynamic sizes and size distributions of the nanocrystals were determined by asymmetrical flow field-flow fractionation (AF4) coupled with a UV–Vis and a dynamic light scattering (DLS) detector. The stability of QDs in limb bud culture medium during the incubation time (one week) was assessed by ICP-MS. Details are provided in the supplemental materials. The properties of QDs used in the current investigations are shown in Figure 1(A)–(E). Fluorescently labeled dPGS-Cy5 (3.5G) dendrimers (Figure 1F) were provided by the research group of Dr Rainer Haag, Freie Universität Berlin (Germany) and were prepared by applying previously reported synthetic procedures. In brief, hydroxyl-terminated dendritic polyglycerol (dPG) was prepared in an anionic ring-opening multibranching polymerization of glycidol on a partially deprotonated trimethylolpropane starter by applying slow monomer addition to suppress undesired cyclization (Dernedde et al., 2010; Sunder et al., 1999, 2000).

Animals

Animal experiments were approved by McGill University and were fully compliant with the guidelines established by the Canadian Council on Animal Care under protocol 1825. Mice were housed in the McIntyre Animal Resource Centre (McGill University, Montreal, QC, Canada) and maintained on a 12-h light/dark cycle with access to food and water *ad libitum*.

Limb bud cultures

Timed-pregnant CD1 mice (20–25 g), mated between 8:00 and 10:00 a.m. (gestation day 0), were purchased from Charles River Canada Ltd (St. Constant, QC, Canada). Triple transgenic *Col2a1*-ECFP, *Col10a1*-mCherry and *Col1a1*-YFP reporter mice on a CD1 background, provided by Dr David L. Butler (University of Cincinnati, Cincinnati, OH) and Dr David Rowe (University of Connecticut Health Center, Farmington, CT), were bred in the McIntyre Animal Centre. Between 8:00 and 10:00 a.m. on gestation day 12, females were euthanized by CO_2 inhalation and cervical dislocation, the uteri were removed and embryos were explanted into Hank's balanced salt solution (HBSS, Life Technologies Inc., Burlington, ON, Canada). The embryonic forelimbs were cultured as previously described (Huang & Hales, 2002; Paradis et al., 2012) and illustrated in Figure 2. Briefly, limbs were excised just lateral to the somites and randomly assigned in equal numbers to the different groups (4–5 limbs per bottle). Limbs were cultured *in vitro* in 6 mL of culture medium consisting of 75% BGJb medium (GIBCO BRL Products, Burlington, ON, Canada), 25% salt solution supplemented with ascorbic acid (160 μg/mL), and gentamicin (1 μL/mL, GIBCO BRL Products). Each culture was gassed with 50% O_2, 5% CO_2 and 45% N_2. Specified concentrations of nanomaterials or vehicle (water) were added to the designated cultures. Sodium valproate (VPA, 3.6 mM, Sigma, St. Louis, MO, no. P4543) served as a positive control for limb defects. The medium was changed after three days of culture; fresh medium did not contain nanoparticles or VPA. The cultures were ended at the specified times.
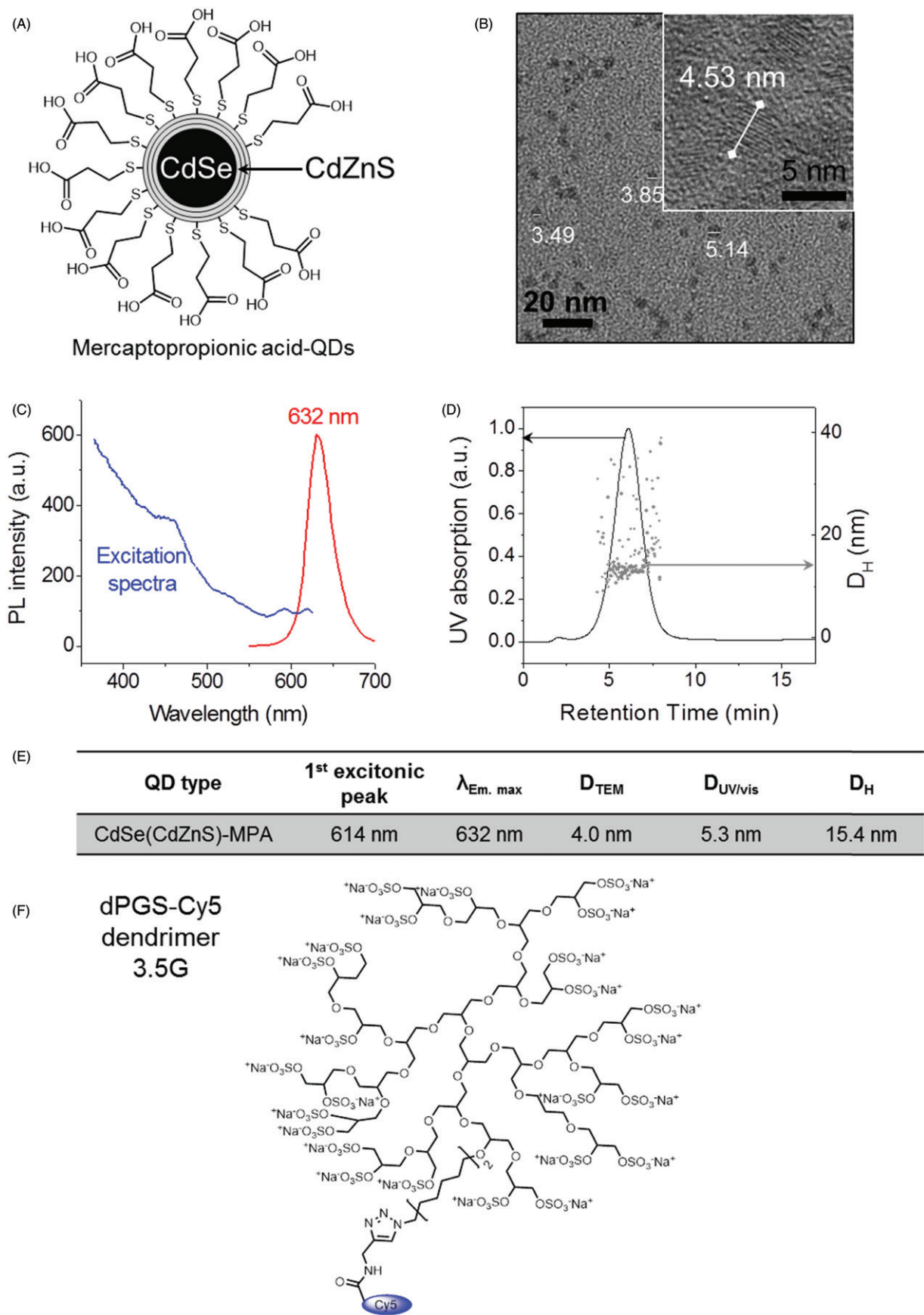
Figure 1. Physicochemical properties of QD-MPA and the structure of dPGS-Cy5. (A) Schematic of QD-MPA with CdSe cores encapsulated in a shell representing approximately three monolayers of CdZnS alloy. Schematic not to scale. (B) TEM micrograph of QD-MPA deposited on a Formvar-coated grid. Inset shows HR-TEM of the same QDs. (C) Luminescence emission spectra of the QD-MPA after excitation at 365 nm and excitation spectra measured for the emission at 632 nm. (D) Fractogram from the AF4 elution of the QD-MPA in 1 mM phosphate buffer. The elution is observed by a UV–Vis detector measuring at 300 nm (in black). The hydrodynamic diameter of the eluting particles is reported on the right *y*-axis. (E) Table of the optical properties of the QD-MPA and the sizes determined by TEM, UV-absorption spectra and the hydrodynamic size determined by AF4 hyphenated with a DLS detector. (F) Structure of dendritic polyglycerol sulfate (dPGS) of generation 3.5 labeled with Cy5 fluorophore.
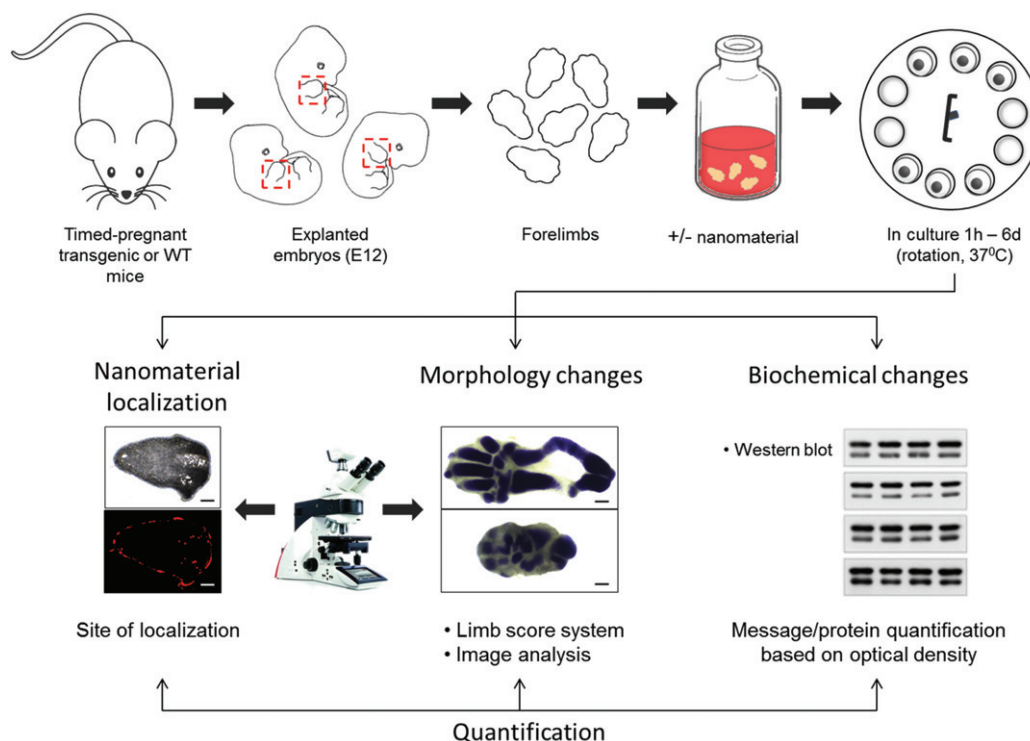
Figure 2. *In vitro* murine limb bud culture system. Timed-pregnant CD1 mice or transgenic reporter mice on day 12 of gestation were euthanized, the uteri were removed and embryos were explanted into HBSS. The embryonic forelimbs were excised just lateral to the somites, pooled and cultured in chemically defined medium in the presence or absence of nanomaterial. The cultures were maintained at 37 °C in continuous rotation. Embryonic limbs were cultured for up to 6 days. The limb bud culture system can be further exploited to quantitatively assess nanomaterial localization in limbs, morphology changes and biochemical changes in limbs caused by nanomaterial exposure. In particular, imaging techniques allow determination of the site of nanomaterial localization in tissues; morphology changes can be quantified using a limb differentiation scoring system or image analysis. RT-PCR and western blot can be employed to assess biochemical changes via message or protein quantification using optical densitometry.

Assessment of nanoparticle uptake

Limbs were treated with QD-MPA or dPGS-Cy5 at the concentrations of 3, 30 or 100 nM in water (equivalent to 1.03, 10.33 or 34.4 mg/L, based on calculated estimations of the molar mass of QDs, or to 45.3 µg/L, 453 µg/L or 1.51 mg/L for dPGS-Cy5); vehicle was added to the control groups. Limbs cultured for 1, 3, 24, 72 h or 6 days were fixed with 4% paraformaldehyde (PFA) for 2 h at 4 °C in the dark, then soaked in a series of sucrose solutions (15% sucrose/PBS/0.2% PFA and 30% sucrose/PBS/0.2% PFA, each for 30 min at 4 °C in the dark). Limbs were embedded in molds filled with Tissue-Tek O.C.T. Compound (Sakura Finetek, Alphen aan den Rijn, The Netherlands) and incubated for 30 min at 4 °C in the dark. Each limb was oriented flat at the bottom of the mold. Cryomolds were flash frozen with acetone added to the dry ice pellets, and tissue blocks were mounted on metal grids. Sections (14 µm) were cut using a Leica CM1850 UV cryostat (Leica Microsystems Inc., Concord, Ontario, Canada), mounted on slides and dried at room temperature in the dark. Images were acquired with a Leica DFC350FX monochrome digital camera connected to a Leica DMI4000B inverted fluorescence microscope for dPGS-Cy5 and with a DFC310FX color digital camera connected to a Leica DM1000 upright microscope for QD-MPA. The fluorescent intensity of nanoparticles was quantified using ImageJ imaging software (NIH, Bethesda, MD). Four to five separate replicates (8–12 limbs per treatment group, 6–12 sections per limb) were done for each treatment and time point.

Limb morphology

Forelimbs cultured for 6 days were fixed with Bouin's fixative overnight, stained with 0.1% toluidine blue (Fisher Scientific,

Nepean, Ontario, Canada) in 70% ethanol for 24 h, dehydrated in an alcohol series (95% and 100% ethanol, 1 h each), and stored in cedarwood oil (Fisher Scientific). Limbs were observed using a dissection microscope and the morphology and differentiation of each limb was assessed using a limb morphogenetic differentiation scoring system (Neubert & Barrach, 1977). Briefly, this system attributes a score to the radius, ulna, carpalia and each one of the five digits according to their differentiation status. In addition, computerized image analysis of the cartilage area was used to quantitatively examine cultured limbs. The cartilage area was measured by Image-Pro Premier v9.0 Image Analysis software (Media Cybernetics, Rockville, MD). Four to six separate replicates ($n = 4$–6 bottles for each treatment, with 6–8 limbs per bottle) were done.

Assessment of collagen gene expression

Collagen gene expression was assessed using limbs from the triple transgenic *Col2a1*-ECFP, *Col10a1*-mCherry and *Col1a1*-YFP reporter mice. Limbs from ECFP-positive embryos were treated with QD-MPA or dPGS-Cy5 at concentrations of 30 or 100 nM and cultured for 6 days; vehicle (water) or VPA (3.6 mM) exposed limbs served as controls. The fluorescence signals of the biomarkers of differentiation were observed after 6 d in culture; fluorescence images were acquired with a Leica DFC450C color digital camera connected to a Leica M165 FC fluorescent stereomicroscope. The experiment was repeated twice.

Western blot analysis

After a 24 h culture period, limbs were homogenized by sonication in lysis buffer containing protease inhibitors: 150 mM
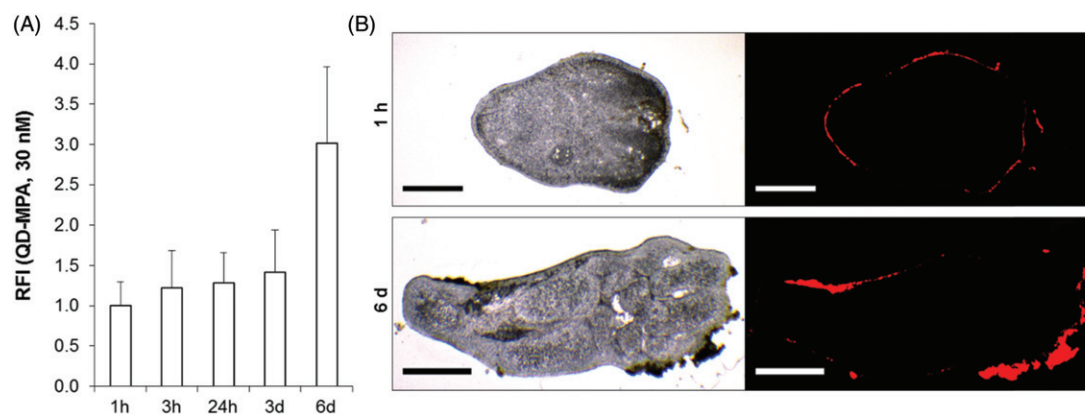
Figure 3. The fluorescence signal of QD-MPA detected in limb sections increased in a time-dependent manner. Embryonic day-12 forelimbs were treated with 30 nM of QD-MPA and cultured for 1, 3, 24 h, 3 d or 6 d. Limbs were fixed and then sectioned using a cryosectioning technique. (A) Relative fluorescence intensities compared with 1 h were quantified from fluorescent microscopy pictures. Data are presented as means ± SEM of 4–5 separate experiments (in total 9–10 limbs per group). The Mann–Whitney *U*-test and a *post-hoc* Bonferroni correction were done. (B) Representative microscopy pictures; QD-MPA are visible in red and occur only at the surface of the limb sections. Scale bars = 0.3 mm.

NaCl, 1% Nonidet P-40, 0.5% sodium deoxycholate, 0.1% SDS, 50 mM Tris pH 7.5, 40 µg/mL bestatin, 0.2 M phenylmethylsulfonyl fluoride, 10 µg/mL leupeptin and 6 µg/mL aprotinin. Total protein was extracted and quantified using spectrophotometric Bio-Rad protein assays (Bio-Rad Laboratories, Mississauga, Ontario, Canada). Proteins (15–20 µg per sample) were separated by 15% SDS-PAGE and transferred to equilibrated polyvinylidene difluoride membranes (Amersham Biosciences, Division of GE Healthcare Life Sciences, Baie D-Urfe, Québec, Canada) by electroblotting. Precision standards (Bio-Rad Laboratories) were used as molecular weight markers. Membranes were blocked in 5% nonfat milk in Tris-buffered saline with Tween 20 (TBS-T) (137 mM NaCl, 20 mM Tris pH 7.4, 0.05% Tween 20) for 1 h at room temperature, and then probed overnight at 4 °C with primary antibodies, washed and incubated with the secondary antibody for 2 h at room temperature. Immunoblotting was done using polyclonal antibodies against cleaved caspase-3 (1:1000; Cell Signaling Technology Inc., Danvers, MA, Catalog no. 9661L), Bax (1:1000; Santa Cruz Biotechnology Inc., Santa Cruz, CA, Catalog no. sc-526), Bcl-2 (1:1000; Santa Cruz Biotechnology Inc., Santa Cruz, CA, Catalog no. sc-492), proliferating cell nuclear antigen (PCNA) (1:2500; Santa Cruz Biotechnology Inc., Catalog no. sc-56) and β-actin (1:10 000; donkey polyclonal IgG, Santa Cruz Biotechnology Inc., Catalog no. sc-1616). The secondary antibodies, conjugated to horseradish peroxidase, were donkey anti-rabbit antibodies (1:5000; GE Healthcare Limited, Catalog no. NA934) for cleaved caspase-3, Bax, Bcl-2, and PCNA and anti-goat antibodies (1:10 000; Santa Cruz Biotechnology Inc., Catalog no. sc-2056) for β-actin. Proteins were visualized with the Enhanced Chemiluminescence Plus Kit (Amersham Biosciences). Protein bands were quantified by densitometric analysis using a Chemi-Imager 400 Imaging system (Alpha Innotech, San Leandro, CA). Five separate replicates were done for each experiment; values represent means ± SEM.

Statistical analyses

Data were checked for normality and homogeneity of variances to determine the appropriate statistical method. One-way analysis of variance (ANOVA) followed by a *post-hoc* Bonferroni's correction for multiple comparisons was used to compare the levels of protein expression against controls using Systat 10.2 (Systat Software, Point Richmond, CA). Data for fluorescence intensities

did not meet the requirements for the use of parametric methods; therefore, the Mann–Whitney test with Bonferroni's correction for multiple comparisons was used. Statistical significance was assumed with $p < 0.05$.

Results

Characterization of nanomaterials

The CdSe/CdZnS nanocrystals (schematic representation in Figure 1A) were prepared in organic solvents and modified with MPA to suspend them in aqueous media. The TEM results (Figure 1B) show the small size of the nanocrystals as well as the crystalline structure of the surface of the QDs as prepared in organic solvent. The size distribution of the surface-modified QDs can be visualized by the narrow emission spectra which has a full width at half-maximum equal to 33 nm (Figure 1C). The size distribution of the suspended QD-MPA was also measured by asymmetrical flow field-flow fractionation (AF4) in PBS. The average hydrodynamic diameter of the QDs was equal to 15.4 nm (Figure 1D and E). The structure of dendritic polyglycerol sulfate (dPGS) of generation 3.5 labeled with Cy5 fluorophore is depicted in Figure 1(E).

Nanomaterials are localized at the limb bud surface

During the culture period limbs differentiate on three axes: proximal–distal, cranial–caudal and dorsal–ventral. To evaluate the distribution of nanomaterials in limb tissues, limbs were exposed to QD-MPA or dPGS-Cy5 at various concentrations (3–100 nM) for 1, 3, 24 h, 3 d or 6 d (Figures 3–6). Limbs were cryosectioned and then imaged using fluorescence microscopy. Our results showed that the fluorescence signal of QD-MPA (Figure 3A) and dPGS-Cy5 (Figure 5A) increased over time; the fluorescence signals detected in cryosections after 6-day treatments with either QD-MPA or dPGS-Cy5 were markedly increased compared with limbs cultured for 1 h. Changes in relative fluorescence intensity (RFI) were concentration-dependent for both QD-MPA (Figure 4A) and dPGS-Cy5 (Figure 6A), with a significant difference ($p < 0.001$) in limb buds exposed to concentrations ≥30 nM.

The limb buds were continuously shaken during the incubation period, allowing the exposure of suspended nanoparticles to different tissue sites. Fluorescence microscopy revealed that QD-MPA were adsorbed and visible at the surface of the limb
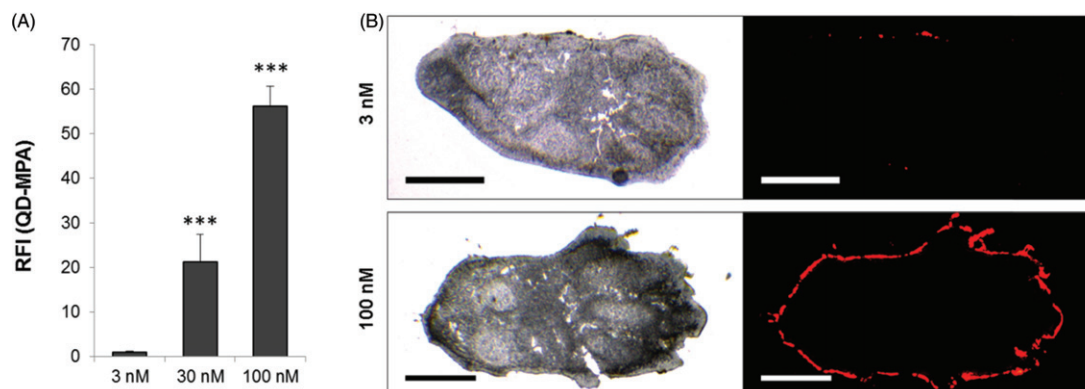
Figure 4. The fluorescence signals of QD-MPA detected in limb sections increase in a concentration-dependent manner. Embryonic day-12 forelimbs were cultured in the presence of increasing concentrations of QD-MPA (3, 30 or 100 nM) for 24 h. They were fixed and then sectioned using a cryosectioning technique. (A) Fluorescence intensity was quantified from fluorescent microscopy pictures. Data are presented as means ± SEM of 4–5 separate experiments (in total 9–10 limbs per group). The Mann–Whitney *U*-test and a *post-hoc* Bonferroni correction were done. Asterisks denote a statistically significant difference ($p < 0.001$ versus 3 nM treatment group). (B) Representative microscopy pictures; QD-MPA are visible in red and occur only at the surface of the limb sections. Scale bar = 0.3 mm.
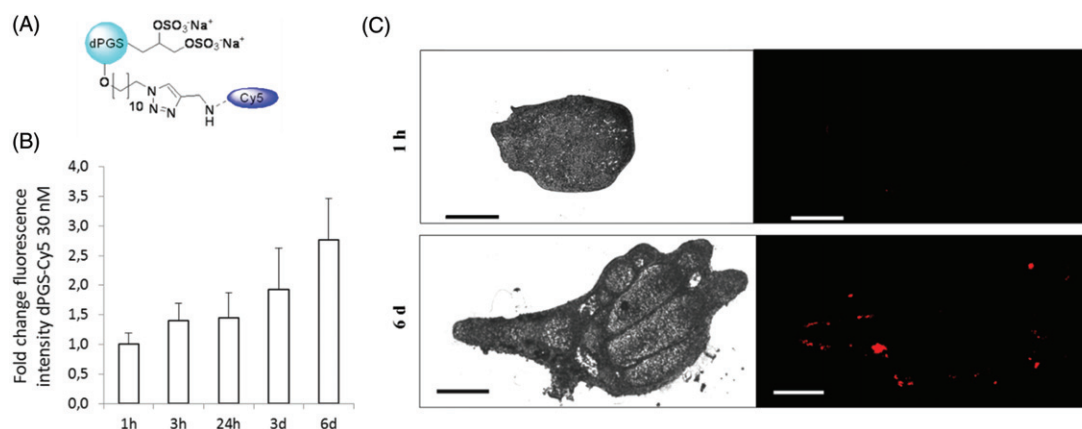

Figure 5. The fluorescence signals of dPGS-Cy5 detected in limb sections increase in a time-dependent manner. Embryonic day-12 forelimbs were treated with 30 nM of dPGS-Cy5 and cultured for 1, 3, 24 h, 3 d or 6 d. Limbs were fixed and then sectioned using a cryosectioning technique. (A) Relative fluorescence intensities compared with 1 h were quantified from fluorescent microscopy pictures. Data are presented as means ± SEM of 4–5 separate experiments (in total 9–10 limbs per group). The Mann–Whitney *U*-test and a *post-hoc* Bonferroni correction were done. (B) Representative microscopy pictures; dPGS-Cy5 are visible in red and occur only at the surface of the limb sections. Scale bar = 0.3 mm.

sections after 1 h of exposure (Figures 3B and 4B); even after 6 days in culture no fluorescence was detected inside the limb sections. Similarly, dPGS-Cy5 dendrimer signals were detected only on the limb surfaces (Figures 5B and 6B). These findings suggest that the skin of the developing limbs limits the internalization of QD-MPA nanocrystals and fluorescent dendrimers. However, the possibility that nanostructures are taken up in minute quantities, below the detection limit of fluorescence microscopy, remains. Additional experiments were done to investigate the morphological and biochemical consequences of exposure to these nanoparticles.

Limb morphology and differentiation are only affected by high QD-MPA concentrations

Embryonic forelimbs were cultured in the presence or absence of QD-MPA or dPGS-Cy5 to investigate whether exposure to the particles during limb development affects morphology and differentiation. The consequences of QD-MPA and dPGS-Cy5 exposures were compared with those induced by VPA. Representative limbs stained with toluidine blue are shown in Figure 7(A). Toluidine blue stains the proteoglycans and glycosaminoglycans of the extracellular matrix in cartilage and

is commonly used as an indicator of late chondrogenesis. The control limbs demonstrated normal differentiation of the anlagen of the long bones and digits. A radius, ulna, carpals, five metacarpals and phalanges were observed after 6 days in culture. The low (3 nM) and middle concentration (30 nM) QD-MPA treatment groups showed minor effects on morphology, whereas the limbs exposed to 100 nM QD-MPA exhibited marked decreases in growth and differentiation that were similar to those induced by VPA. The overall size of the forelimbs was reduced, the long bones and metacarpals were short and thick, and phalanges were often missing. In some instances, complete absence of one or more metacarpals, also known as oligodactyly, was observed. In contrast, limbs exposed to dPGS-Cy5 (3, 30 or 100 nM) were not different from control limbs (Figure 7A). The morphology and state of differentiation of the limbs was assessed quantitatively using a limb morphogenetic differentiation scoring system (Figure 7B) or two-dimensional measurement of the cartilage area (Figure 7C). While limbs exposed to dPGS-Cy5 (3, 30 or 100 nM) were not different from control limbs (Figure 7B and C), significant decreases in the limb score and cartilage area were observed in limbs treated with 100 nM QD-MPA. Thus, the high concentration of QD-MPA inhibited limb development *in vitro* and caused a pronounced decrease in cartilage formation.
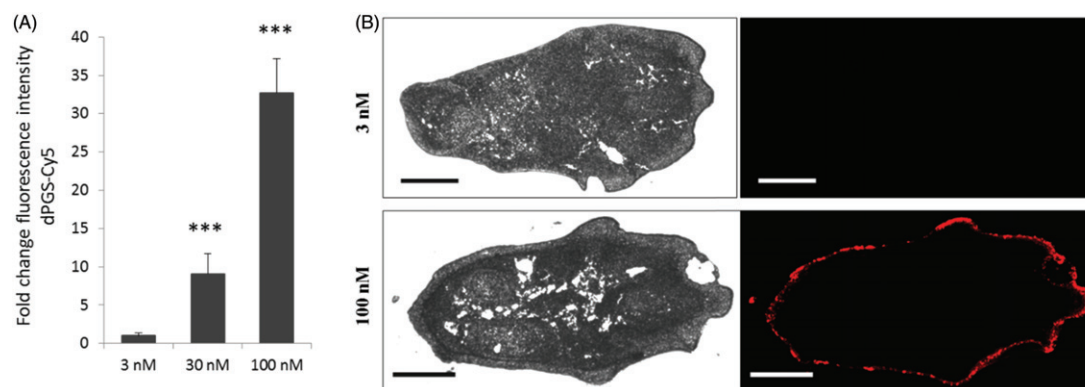
Figure 6. The fluorescence signals of dPGS-Cy5 detected in limb sections increased in a concentration-dependent manner. Embryonic day-12 forelimbs were cultured in the presence of increasing concentrations of dPGS-Cy5 (3, 30 or 100 nM) for 24 h. They were fixed and then sectioned using a cryosectioning technique. (A) Fluorescence intensity was quantified from fluorescent microscopy pictures. Data are presented as means ± SEM of 4–5 separate experiments (in total 9–10 limbs per group). The Mann–Whitney *U*-test and a *post-hoc* Bonferroni correction were done. Asterisks denote a statistically significant difference (*p* < 0.001 versus 3 nM treatment group). (B) Representative microscopy pictures; dPGS-Cy5 are visible in red and occur only at the surface of the limb sections. Scale bar = 0.3 mm.
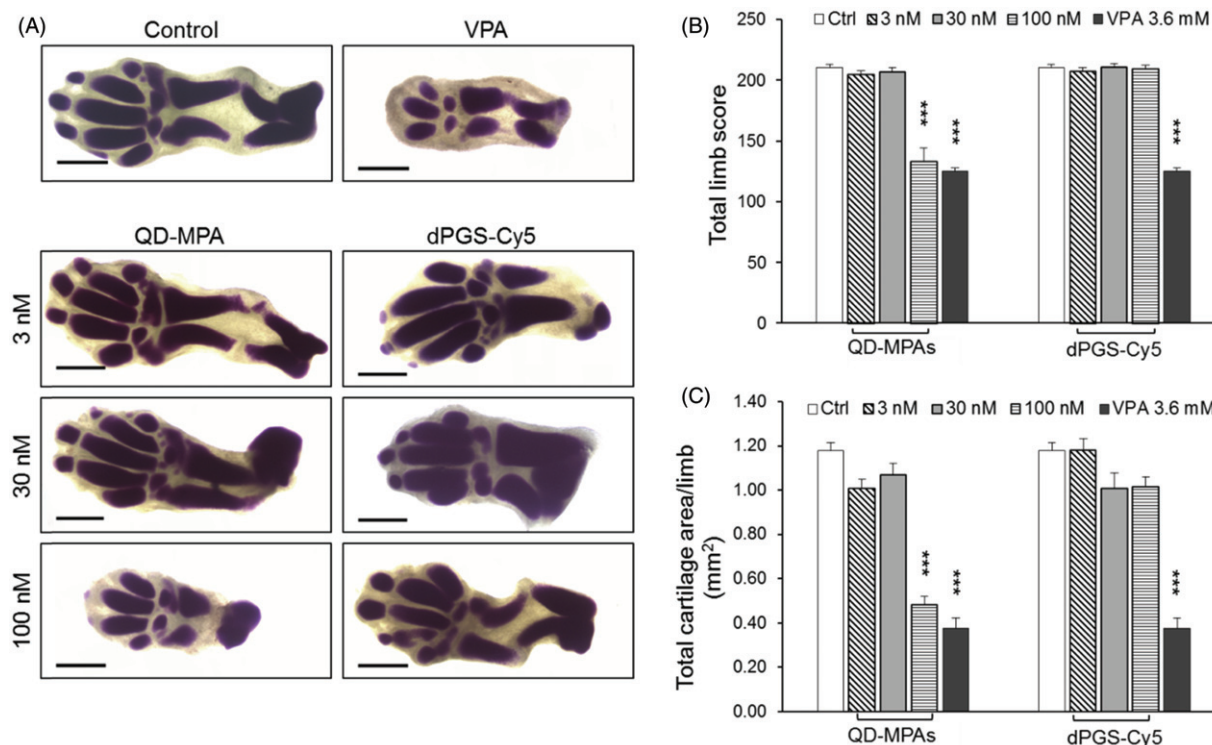

Figure 7. The effects of QD-MPA and dPGS-Cy5 on limbs. Embryonic day-12 forelimbs were cultured in the presence of QD-MPA or dPGS-Cy5 (3, 30 or 100 nM) for 6 days. VPA (3.6 mM) was used as a positive control. Limbs were fixed and stained with 0.1% toluidine blue (A) to visualize cartilage formation. The extent of limb differentiation was assessed using morphogenetic differentiation scoring system (B), and the limb growth was assessed by determining the two-dimensional cartilage area (C). Exposure to the high concentration of QD-MPA had marked effects on chondrogenesis, in particular on digit formation. Scale bar in (A) (applies to all) = 0.5 mm. Data are expressed as means ± SEM from 3 to 4 separate experiments (*n* = 20–25 limbs/group). The Mann–Whitney *U*-test for (B) and one-way ANOVA for (C) followed by *post-hoc* Bonferroni correction were done. Asterisks denote a statistically significant difference (*p* < 0.001 versus the control group).

Markers of chondrogenesis and osteogenesis are altered by QD-MPA

The similarity of limb development defects caused by exposure to the high concentration of QD-MPA and to VPA (Figure 7A) suggested that QD-MPA may interfere with chondrogenesis and osteogenesis during cartilage formation. To determine whether these processes were disrupted after nanoparticle exposure, we used transgenic mice that report the expression patterns of the *Col2a1*:ECFP, *Col10a1*:mCherry and *Col1a1*:YFP transgenes. Forelimbs of transgenic embryos treated with vehicle (water), the medium concentration of QD-MPA, or with the medium or high concentrations of dPGS-Cy5, and cultured for 6 days, showed an expression domain of the three transgenes (Figure 8), indicating that cartilage differentiation was proceeding normally.
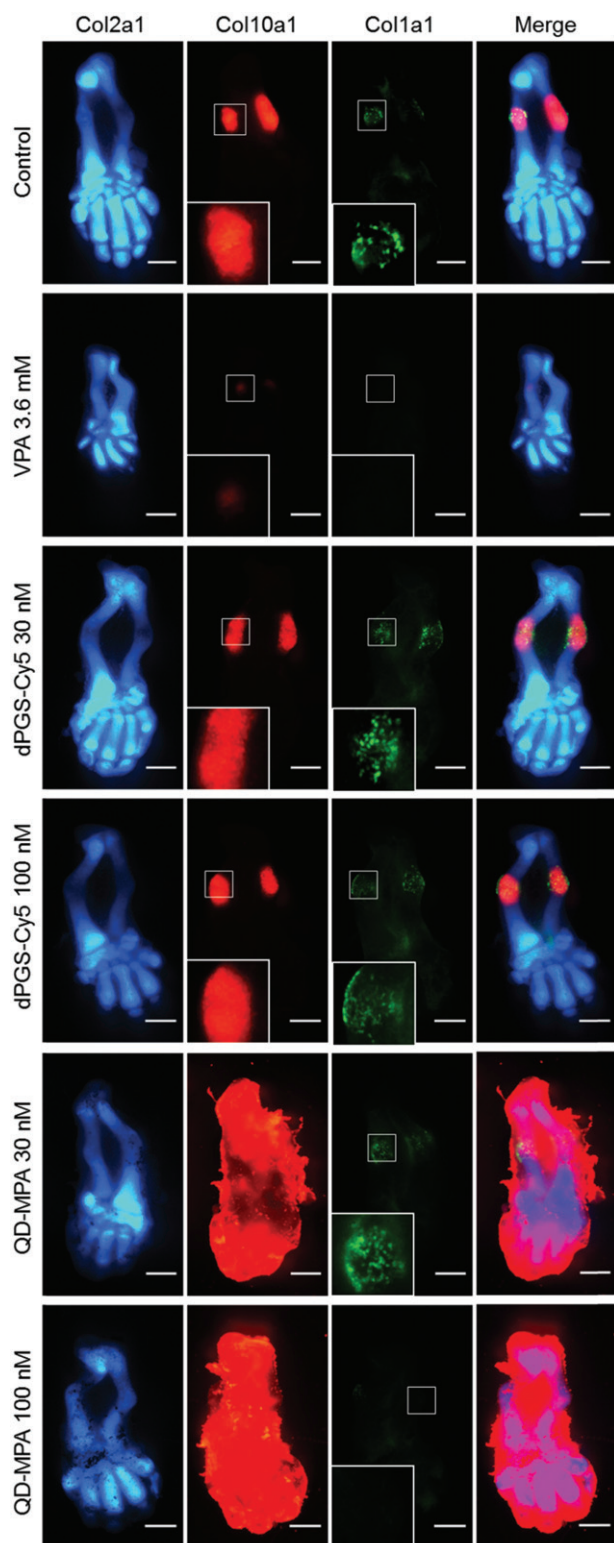
Figure 8. Expression of molecular markers of chondrogenesis and osteogenesis. Limbs of transgenic embryos were treated with vehicle (water), VPA (3.6 mM), dPGS-Cy5 (30 or 100 nM) or QD-MPA (30 or 100 nM) and imaged after 6 days in culture. QD-MPA tend to stick to the surface of the limbs, thus, disrupting a fluorescence signal of the *Col10a1*:mCherry transgene. Scale bar (applies to all) = 0.5 mm.

As indicated by the uptake studies, QD-MPA accumulated on the surface of the limbs exposed to the high concentration. The fluorescence signal of QD-MPA overlapped with that of *Col10a1*:mCherry transgene, thus, preventing the visualization of COL10A1 expression (Figure 8). To overcome this problem, we cryosectioned the treated limbs and, therefore, present merged

images of the QD-MPA-treated limb sections (Figure 9). The images of the limb sections for all treatment groups are provided in supplementary material (Figure S1). In contrast to dPGS-Cy5, limbs treated with the high concentration of QD-MPA showed markedly diminished expression domains of the three markers: *Col2a1:ECFP*, *Col10a1*:mCherry and *Col1a1*:YFP that were comparable to the effects of VPA (Figure 8).

Markers of apoptosis and proliferation are not markedly affected by the selected nanomaterials

Proliferation and apoptosis are key processes in normal limb development; proliferation is crucial for limb outgrowth and cartilage extension whereas apoptosis plays a pivotal role in the interdigital tissue cell death and digit separation. We examined the effects of exposure to medium or high concentrations of QD-MPA or dPGS-Cy5 on the expression of PCNA and on the expression of markers of apoptosis, in particular, cleaved caspase-3, BAX and BCL-2, in embryonic forelimbs. PCNA protein was detected in control limbs 24 h after the initiation of culture. None of the performed treatments altered PCNA protein concentrations in limbs (Figure 10A and B). Western blot analysis revealed that the levels of cleaved caspase-3, BCL-2 and BAX proteins were not significantly affected after 24 h exposure to either the QD-MPA or the dPGS-Cy5 dendrimers (Figure 10C and D), although exposure to QD-MPA resulted in a trend toward a concentration-dependent increase in cleaved caspase-3. Although the expression of BCL-2 was visibly upregulated after dPGS-Cy5 exposure compared with the control group, the BCL-2/BAX ratio was not affected. Thus, the QD-MPA-induced reductions in limb growth and differentiation were not associated with effects on PCNA expression, cleaved caspase-3, BAX or BCL-2.

Discussion

Using the limb bud culture model, we show that QD-MPA causes concentration-dependent pronounced morphological changes in limb growth and differentiation. In contrast, dPGS-Cy5 do not show any adverse effects on limb development within the same time period at any of the concentrations tested. Evidence is accumulating that inhaled nano-sized particles may translocate across cell membranes into the circulation and accumulate in various organs (Kreyling et al., 2013). Neonates from timed pregnant CD1 mice that were exposed to cadmium oxide nanoparticles by inhalation had significantly elevated cadmium levels on post-natal days 1–5 (Blum et al., 2012). The *in vivo* studies of QD in pregnant mice showed that intravenously administered QDs were detected mainly in the dam liver and spleen soon after injection (Lin et al., 2008; Su et al., 2011; Tiwari et al., 2011; Yang et al., 2007; Yeh et al., 2011). QDs that were injected (intravenously) into pregnant mice toward the end of gestation crossed the placental barrier and reached fetal tissues (Chu et al., 2010). These studies provide useful information on the effects of QD size, dosage and capping material properties in influencing the ability of QDs to cross the placenta; however, the possible morphological and biochemical changes in embryos as a consequence of QD exposure were not investigated.

In the current study, we employed the limb bud culture system to assess the effects of QD-MPA and dPGS-Cy5 during organogenesis. Results from these studies show the usefulness of model nanomaterials of similar sizes (approximately 5–10 nm) for comparison in toxicological screening. Limb bud cultures allowed testing of the nanomaterials for a prolonged time periods (6 days) which are often not possible in rapidly proliferating cells in monolayers. The key finding from our studies is that despite very limited penetration of QD-MPA into the limb tissue, readily detectable cartilage deformation and differentiation defects were
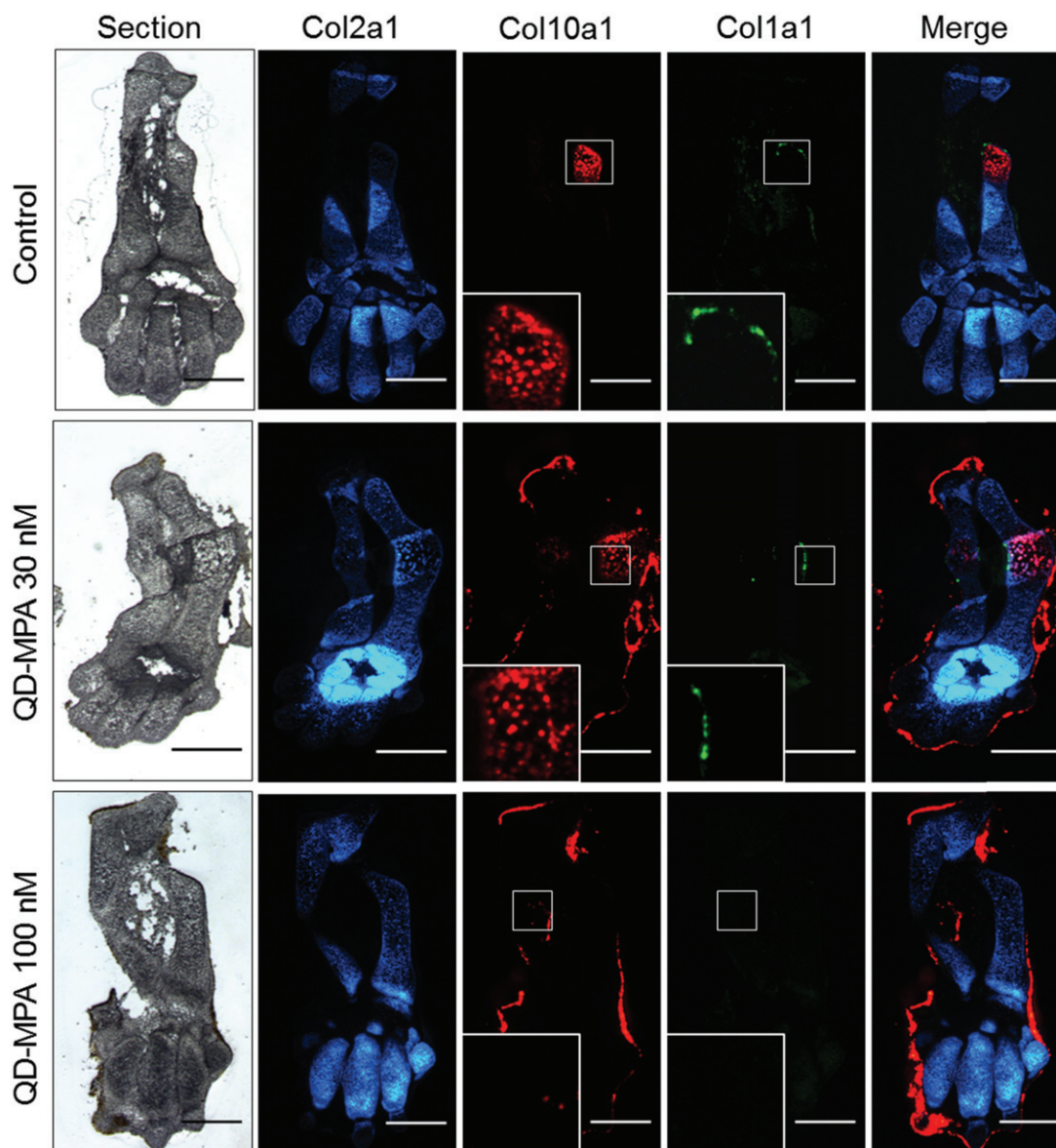
Figure 9. Expression of molecular markers of chondrogenesis and osteogenesis in limb cryosections. Limbs of transgenic embryos were cultured for 6 days in the presence of vehicle (water) or QD-MPA (30 or 100 nM), then limbs were cryosectioned and imaged using fluorescence microscopy. Limbs treated with 100 nM QD-MPA showed reduced expression of *Col1a1* and *Col10a1*. Scale bar (applies to all) = 0.5 mm.

observed. Toluidine blue staining and *Col2a1* reporter mice revealed severe limb reduction and inhibition of cartilaginous anlagen differentiation in mouse embryonic forelimbs. These effects were concentration-dependent within the 30–100 nM range and were comparable to those of a model teratogen, VPA. In contrast, exposure to the equivalent concentrations (3–100 nM) of dPGS-Cy5 had no visible effects on limb morphology. To interpret these findings in a risk assessment context it would be important to compare the concentrations tested in this *ex vivo* model system with the expected levels of human exposure.

Similar to gold and some other nanoparticles (Kreyling et al., 2013), only a small fraction of QDs would cross biological barriers and reach the limb buds after *in vivo* administration (Kreyling et al., 2013). Thus, exposure of limb buds to 100 nM QD concentrations seems to be excessively high. However, repeated experiments with low QD concentrations up to 50 nM did not reveal any measurable morphological or biochemical changes under experimental conditions employed in our studies. Limb buds exposed to higher QD concentrations (100 nM) were able to cause some malformations. Exceedingly high doses of stable and protected QDs were necessary to reveal measurable

and significant undesirable effects. That such QDs in low nanomolar concentrations do not cause readily detectable malformations indicates that they could be used in experimental animals. Results from our studies clearly show that stable and well-characterized QDs when used in low nanomolar concentrations (<50 nM) can be used for basic science research and that 3D limb bud cultures are suitable for toxic screening of new nanomaterials.

Chondrogenesis, or cartilage formation, is a tightly regulated multi-step event during which chondrocytes undergo sequential proliferation, differentiation and hypertrophy. Each of these steps is characterized by the expression of specific molecular markers. Type II collagen (COL2A1) is found in early proliferative (immature) chondrocytes and is essential for cartilage extracellular matrix formation (Akiyama et al., 2002; Bi et al., 2001). The type X collagen gene (*Col10a1*) is specifically expressed in hypertrophic chondrocytes and is regulated by RUNX2, the master transcription factor of maturing chondrocytes and developing osteoblasts (Ding et al., 2012). Type I collagen (COL1A1) is a major marker for osteogenic differentiation (Stacey et al., 1988). Limbs treated with the high concentration of QD-MPA showed an
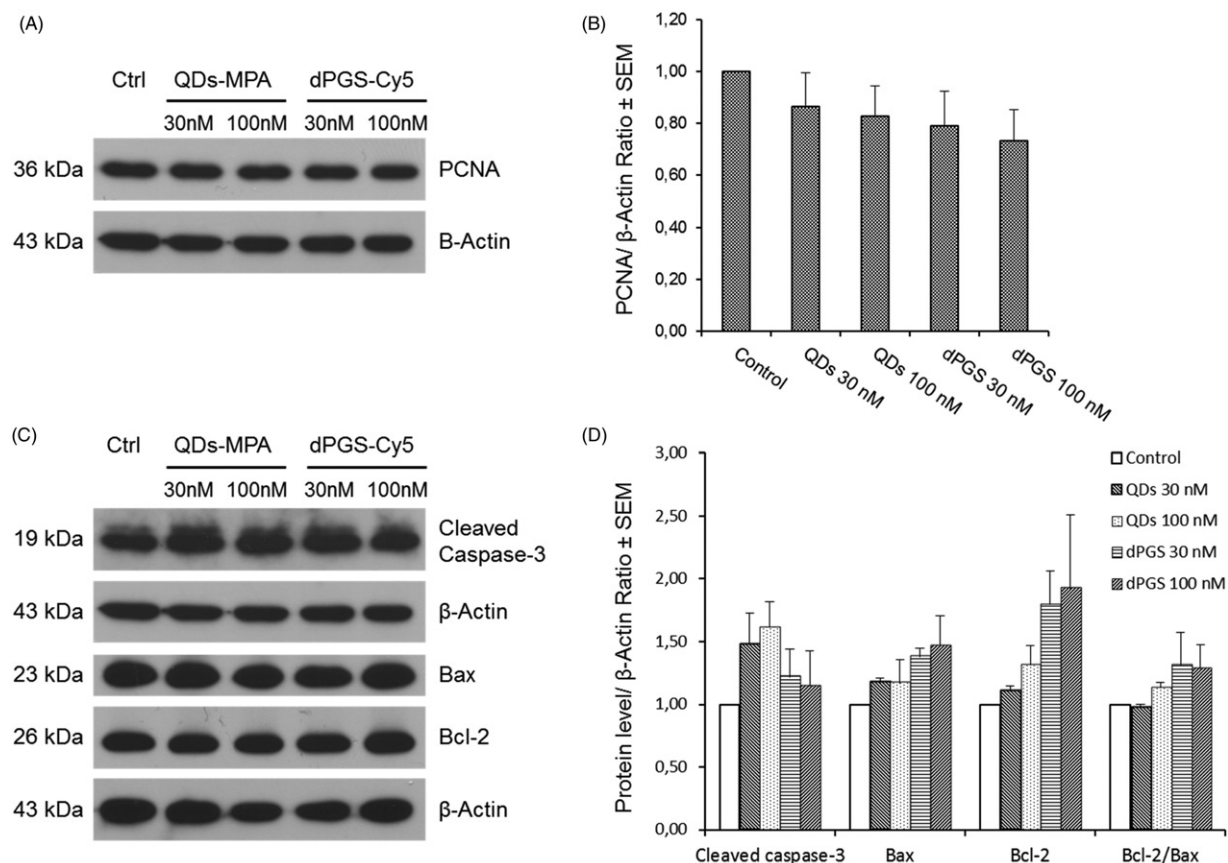
Figure 10. Exposure to medium or high concentrations of QD-MPA or dPGS-Cy5 did not affect the expression of markers of proliferation or apoptosis. (A, C) Western blot analysis of PCNA, cleaved caspase-3, BAX and BCL-2 in the mouse forelimbs cultured for 24 h in the presence of vehicle (water), QD-MPA (30 or 100 nM) or dPGS-Cy5 (30 or 100 nM). PCNA, cleaved caspase-3, BAX and BCL-2 were detected as 36, 19, 23, and 26 kDa bands, respectively. (B, D) Densitometric analysis of the bands normalized to β-actin. Results were normalized to the control. Data are expressed as means ± SEM ($n = 5$ with 7–8 limbs per sample). One-way ANOVA and a *post-hoc* Bonferroni correction were done (applied to all).

inhibitory effect on COL10A1 and COL1A1 expression in addition to an effect on growth. These observations suggest that exposure to QD-MPA causes defects or delays in the processes of matrix mineralization and ossification in cultured limbs. Although chondrogenesis is completed before adulthood, bone resorption and deposition are dynamic processes throughout life. Furthermore, limb chondrogenesis involves pathways and regulators that are identical to those in the ribs and the axial skeleton. Hence, these results suggest that exposure to QDs during organogenesis may impair skeletal development and affect embryo health. The underlying molecular mechanism and whether these delays can permanently affect the skeletal bone density and fragility remain to be investigated.

To explore the mechanism of QD-MPA-induced disruption of limb development, we assessed the expression of markers of proliferation and apoptosis in treated limbs. Cell proliferation plays an important role in normal limb development; proliferation is responsible for bone elongation and limb outgrowth. In this study, we used PCNA as a marker to assess cell proliferation in limbs treated with QD-MPA or dPGS-Cy5. We demonstrated that neither QD-MPA nor dPGS-Cy5 altered the expression of PCNA in limbs after 24 h exposure. Thus, the QD-mediated reduction in cartilage formation is unlikely to be associated with impaired cell proliferation processes. In contrast to our findings, Chan & Shiao (2008) demonstrated that in mouse blastocyst-stage embryos, directly treated with QDs for 24 h, CdSe-core QDs inhibited cell proliferation and induced apoptosis. In accord with Chan and Shiao, our results support the protective role of ZnS on the CdSe-core. As suggested previously, the toxic effects of QDs may be

attributable to the nanostructure *per se* or the leakage of cadmium from the QDs. Our ICP-MS data suggest that the toxic effects of QDs (>30 nM) derive from the nanostructures and not from dissolved cadmium which was equal to 0.18 μM for 100 nM of QD-MPA after 1 day incubation in the limb bud culture media at 37 °C. Concentrations up to 5 μM of cadmium chloride were not previously reported to be toxic to HEK293 cells (Chen et al., 2012). The maximum concentration of MPA on QD surfaces (for 100 nM QDs) corresponds to 68 μM MPA, not previously reported as toxic. MPA in high micromolar concentrations (>500 μM) can induce seizures *in vivo* (Crick et al., 2014). It is likely that the increased incidence in cleft palate observed after the administration of repeated high doses of MPA to mice were also due to maternal toxicity, manifested as mild seizures and a decrease in body weight gain (Ding et al., 2004).

Interference with apoptosis may be an important mechanism of action of teratogens that cause limb malformations (Alles & Sulik, 1989; Kurishita, 1989; Ritter et al., 1973). In our study, we examined changes in the expression levels of apoptosis markers and regulating proteins, cleaved caspase-3, BAX and BCL-2. In general, apoptosis can be divided into two major pathways: the extrinsic and intrinsic pathways. Both pathways commonly lead to caspase-3 activation (Youle & Strasser, 2008). It is thought that the sensitivity of cells to the intrinsic apoptotic stimulus is determined by the relative ratio of pro-apoptotic and anti-apoptotic members of the BCL-2 family (Yang & Korsmeyer, 1996). Thus, the ratio between anti-apoptotic and pro-apoptotic proteins, such as BCL-2/BAX, may play a critical role in cell fate. Our results showed that neither QD-MPA nor dPGS-Cy5 caused

overall significant changes in expression of proteins related to apoptosis in treated limbs after 24 h. Nevertheless, there was a trend toward an increase in cleaved caspase-3 protein levels in limbs exposed to a high dose of QDs. The extrinsic pathway of apoptosis, rather than mitochondrial, may mediate the embryotoxicity of QDs since the BCL-2/BAX ratio was not affected. Moreover, other generations of QDs are known to induce the production of ROS. Both ROS and oxidative stress have been shown to play a role in many teratogen-induced malformations, including those of VPA (Gnanabakthan & Hales, 2009; Tung & Winn, 2011). The role of ROS in QD-induced limb dysgenesis remains to be investigated in future studies.

Altogether this study provides valuable evidence for the embryotoxic effects of QDs during mouse embryonic limb development. We showed that QDs inhibit limb differentiation, as assessed by markers of cartilage formation, while deregulation of proliferation or apoptosis is unlikely to occur. While culturing limb buds directly in medium containing a test nanomaterial ignores the possible influence of maternal pharmacokinetics, placental transfer, embryonic distribution, prenatal drug metabolism in the embryo and elimination of the xenobiotic from the organism (Kochhar, 1983), it does permit determination of the consequences of direct exposure to nanomaterials. Elucidation of the underlying molecular pathways that are pivotal during development and may be targeted by nanomaterials is one step toward achievement of an important goal, the development of safe nanomaterials for biomedical purposes.

References

Agashe HB, Dutta T, Garg M, Jain NK. 2006. Investigations on the toxicological profile of functionalized fifth-generation poly(propylene imine) dendrimer. J Pharm Pharmacol 58:1491–8.

Akiyama H, Chaboissier MC, Martin JF, Schedl A, De Crombrugghe B. 2002. The transcription factor Sox9 has essential roles in successive steps of the chondrocyte differentiation pathway and is required for expression of Sox5 and Sox6. Genes Dev 16:2813–28.

Albertazzi L, Gherardini L, Brondi M, Sulis Sato S, Bifone A, Pizzorusso T, et al. 2012. *In vivo* distribution and toxicity of PAMAM dendrimers in the central nervous system depend on their surface chemistry. Mol Pharm 10:249–60.

Al-Hajaj NA, Moquin A, Neibert KD, Soliman GM, Winnik FM, Maysinger D. 2011. Short ligands affect modes of QD uptake and elimination in human cells. ACS Nano 5:4909–18.

Alivisatos AP, Gu W, Larabell C. 2005. Quantum dots as cellular probes. Annu Rev Biomed Eng 7:55–76.

Alles AJ, Sulik KK. 1989. Retinoic-acid-induced limb-reduction defects: perturbation of zones of programmed cell death as a pathogenetic mechanism. Teratology 40:163–71.

Beyerle A, Irmler M, Beckers J, Kissel T, Stoeger T. 2010. Toxicity pathway focused gene expression profiling of PEI-based polymers for pulmonary applications. Mol Pharm 7:727–37.

Bi W, Huang W, Whitworth DJ, Deng JM, Zhang Z, Behringer RR, et al. 2001. Haploinsufficiency of Sox9 results in defective cartilage primordia and premature skeletal mineralization. Proc Natl Acad Sci USA 98:6698–703.

Blum JL, Xiong JQ, Hoffman C, Zelikoff JT. 2012. Cadmium associated with inhaled cadmium oxide nanoparticles impacts fetal and neonatal development and growth. Toxicol Sci 126:478–86.

Calderón M, Quadir MA, Sharma SK, Haag R. 2010. Dendritic polyglycerols for biomedical applications. Adv Mater 22:190–218.

Chan W-H, Shiao N-H. 2008. Cytotoxic effect of CdSe quantum dots on mouse embryonic development. Acta Pharmacol Sin 29:259–66.

Chatterjee K, Sarkar S, Jagajjanani Rao K, Paria S. 2014. Core/shell nanoparticles in biomedical applications. Adv Colloid Interface Sci 209:8–39.

Chen N, He Y, Su Y, Li X, Huang Q, Wang H, et al. 2012. The cytotoxicity of cadmium-based quantum dots. Biomaterials 33:1238–44.

Choi AO, Brown SE, Szyf M, Maysinger D. 2008. Quantum dot-induced epigenetic and genotoxic changes in human breast cancer cells. J Mol Med (Berl) 86:291–302.

Choi AO, Cho SJ, Desbarats J, Lovrić J, Maysinger D. 2007. Quantum dot-induced cell death involves Fas upregulation and lipid peroxidation in human neuroblastoma cells. J Nanobiotechnol 5:1.

Chu M, Wu Q, Yang H, Yuan R, Hou S, Yang Y, et al. 2010. Transfer of quantum dots from pregnant mice to pups across the placental barrier. Small 6:670–8.

Crick EW, Osorio I, Frei M, Mayer AP, Lunte CE. 2014. Correlation of 3-mercaptopropionic acid induced seizures and changes in striatal neurotransmitters monitored by microdialysis. Eur J Pharm Sci 57:25–33.

Derfus AM, Chan WCW, Bhatia SN. 2003. Probing the cytotoxicity of semiconductor quantum dots. Nano Lett 4:11–18.

Dernedde J, Rausch A, Weinhart M, Enders S, Tauber R, Licha K, et al. 2010. Dendritic polyglycerol sulfates as multivalent inhibitors of inflammation. Proc Natl Acad Sci USA 107:19679–84.

Ding M, Lu Y, Abbassi S, Li F, Li X, Song Y, et al. 2012. Targeting Runx2 expression in hypertrophic chondrocytes impairs endochondral ossification during early skeletal development. J Cell Physiol 227:3446–56.

Ding R, Tsunekawaa N, Obata K. 2004. Cleft palate by picrotoxin or 3-MP and palatal shelf elevation in GABA-deficient mice. Neurotoxicol Teratol 26:587–92.

Duncan R, Izzo L. 2005. Dendrimer biocompatibility and toxicity. Adv Drug Deliver Rev 57:2215–37.

Ema M, Kobayashi N, Naya M, Hanai S, Nakanishi J. 2010. Reproductive and developmental toxicity studies of manufactured nanomaterials. Reprod Toxicol 30:343–52.

Frey H, Haag R. 2002. Dendritic polyglycerol: a new versatile biocompatible material. Rev Mol Biotechnol 90:257–67.

Friedman, L. 1987. Teratological research using *in vitro* systems. II. Rodent limb bud culture system. Environ Health Perspect 72:211–19.

Gao X, Yang L, Petros JA, Marshall FF, Simons JW, Nie S. 2005. *In vivo* molecular and cellular imaging with quantum dots. Curr Opin Biotechnol 16:63–72.

Gnanabakthan N, Hales BF. 2009. The oxidative stress response is region specific in organogenesis stage mouse embryos exposed to 5-bromo-2′-deoxyuridine. Birth Defects Res A Clin Mol Teratol 85:202–10.

Hong J-S, Kim S, Lee SH, Jo E, Lee B, Yoon J, et al. 2014. Combined repeated-dose toxicity study of silver nanoparticles with the reproduction/developmental toxicity screening test. Nanotoxicology 8:349–62.

Hoshino A, Fujioka K, Oku T, Suga M, Sasaki YF, Ohta T, et al. 2004. Physicochemical properties and cellular toxicity of nanocrystal quantum dots depend on their surface modification. Nano Lett 4:2163–9.

Huang C, Hales BF. 2002. Role of caspases in murine limb bud cell death induced by 4-hydroperoxycyclophosphamide, an activated analog of cyclophosphamide. Teratology 66:288–99.

Jaiswal JK, Mattoussi H, Mauro JM, Simon SM. 2003. Long-term multiple color imaging of live cells using quantum dot bioconjugates. Nat Biotechnol 21:47–51.

Jiang W, Kim BY, Rutka JT, Chan WCW. 2008. Nanoparticle-mediated cellular response is size-dependent. Nat Nanotechnol 3:145–50.

Kainthan RK, Janzen J, Levin E, Devine DV, Brooks DE. 2006. Biocompatibility testing of branched and linear polyglycidol. Biomacromolecules 7:703–9.

Kannan RM, Nance E, Kannan S, Tomalia DA. 2014. Emerging concepts in dendrimer-based nanomedicine: from design principles to clinical applications. J Intern Med [Epub ahead of print]. DOI: 10.1111/joim.12280.

Kauffer FA, Merlin C, Balan L, Schneider R. 2014. Incidence of the core composition on the stability, the ROS production and the toxicity of CdSe quantum dots. J Hazard Mater 268:246–55.

Khandare J, Calderón M, Dagia NM, Haag R. 2012. Multifunctional dendritic polymers in nanomedicine: opportunities and challenges. Chem Soc Rev 41:2824–48.

King Heiden TC, Dengler E, Kao WJ, Heideman W, Peterson RE. 2007. Developmental toxicity of low generation PAMAM dendrimers in zebrafish. Toxicol Appl Pharmacol 225:70–9.

Kochhar DM. (1983). Embryonic organs in culture. In: Johnson EM, Kochhar D, eds. Teratogenesis and Reproductive Toxicology. Berlin Heidelberg: Springer, 301–14.

Kolhatkar RB, Kitchens KM, Swaan PW, Ghandehari H. 2007. Surface acetylation of polyamidoamine (PAMAM) dendrimers decreases cytotoxicity while maintaining membrane permeability. Bioconjug Chem 18:2054–60.

Kreyling WG, Semmler-Behnke M, Takenaka S, Möller W. 2013. Differences in the biokinetics of inhaled nano- versus micrometer-sized particles. Acc Chem Res 46:714–22.

Kurishita A. 1989. Histological study of cell death in digital malformations induced by 5-azacytidine: suppressive effect of caffeine. Teratology 39:163–72.

Lin P, Chen J-W, Chang LW, Wu J-P, Redding L, Chang H, et al. 2008. Computational and ultrastructural toxicology of a nanoparticle, quantum dot 705, in mice. Environ Sci Technol 42:6264–70.

Lovrić J, Cho SJ, Winnik FM, Maysinger D. 2005. Unmodified cadmium telluride quantum dots induce reactive oxygen species formation leading to multiple organelle damage and cell death. Chem Biol 12:1227–34.

Magdolenova Z, Collins AR, Kumar A, Dhawam A, Stone V, Dusinska M. 2014. Mechanisms of genotoxicity. A review of *in vitro* and *in vivo* studies with engineered nanoparticles. Nanotoxicology 8:233–78.

Manke A, Wang L, Rojanasakul Y. 2013. Mechanisms of nanoparticle-induced oxidative stress and toxicity. Biomed Res Int 2013:942916.

Menjoge AR, Rinderknecht AL, Navath RS, Faridnia M, Kim CJ, Romero R, et al. 2011. Transfer of PAMAM dendrimers across human placenta: prospects of its use as drug carrier during pregnancy. J Control Release 150:326–38.

Michalet X, Pinaud FF, Bentolila LA, Tsay JM, Doose S, Li JJ, et al. 2005. Quantum dots for live cells, *in vivo* imaging, and diagnostics. Science 307:538–44.

Neubert D, Barrach H-J. (1977). Techniques applicable to study morphogenetic differentiation of limb buds in organ culture. In: Neubert D, Merker H-J, Kwasigroch TE, et al, eds. Methods in Pre-Natal Toxicology: Evaluation of Embryotoxic Effects in Experimental Animals. Stuttgart: Georg Thieme Publishers, 241–51.

Oberdörster G. 2010. Safety assessment for nanotoxicology and nanomedicine: concepts of nanotoxicology. J Intern Med 267:89–105.

Ornoy, A. 2006. Neuroteratogens in man: an overview with special emphasis on the teratogenicity of antiepileptic drugs in pregnancy. Reprod Toxicol 22:214–26.

Paradis F-H, Hales BF. 2013. Exposure to valproic acid inhibits chondrogenesis and osteogenesis in mid-organogenesis mouse limbs. Toxicol Sci 131:234–41.

Paradis F-H, Huang C, Hales BF. (2012). The murine limb bud in culture as an *in vitro* teratogenicity test system. In: Harris C, Hansen JM, eds. Developmental Toxicology. New York: Humana Press, Springer, 197–213.

Pelaz B, Jaber S, De Aberasturi DJ, Wulf V, Aida T, De La Fuente JM, et al. 2012. The state of nanoparticle-based nanoscience and biotechnology: progress, promises, and challenges. ACS Nano 6:8468–83.

Ritter EJ, Scott WJ, Wilson JG. 1973. Relationship of temporal patterns of cell death and development to malformations in the rat limb. Possible mechanisms of teratogenesis with inhibitors of DNA synthesis. Teratology 7:219–25.

Stacey A, Bateman J, Choi T, Mascara T, Cole W, Jaenisch R. 1988. Perinatal lethal osteogenesis imperfecta in transgenic mice bearing an engineered mutant pro-alpha 1(I) collagen gene. Nature 332:131–6.

Stoccoro A, Karlsson HL, Coppedè F, Migliore L. 2013. Epigenetic effects of nano-sized materials. Toxicology 313:3–14.

Su Y, Peng F, Jiang Z, Zhong Y, Lu Y, Jiang X, et al. 2011. *In vivo* distribution, pharmacokinetics, and toxicity of aqueous synthesized cadmium-containing quantum dots. Biomaterials 32:5855–62.

Sun J, Zhang Q, Wang Z, Yan B. 2013. Effects of nanotoxicity on female reproductivity and fetal development in animal models. Int J Mol Sci 14:9319–37.

Sunder A, Hanselmann R, Frey H, Mülhaupt R. 1999. Controlled synthesis of hyperbranched polyglycerols by ring-opening multi-branching polymerization. Macromolecules 32:4240–6.

Sunder A, Mülhaupt R, Haag R, Frey H. 2000. Hyperbranched polyether polyols: a modular approach to complex polymer architectures. Adv Mater 12:235–9.

Tiwari DK, Jin T, Behari J. 2011. Bio-distribution and toxicity assessment of intravenously injected anti-HER2 antibody conjugated CdSe/ZnS quantum dots in Wistar rats. Int J Nanomedicine 6:463–75.

Tung EWY, Winn LM. 2011. Valproic acid increases formation of reactive oxygen species and induced apoptosis in postimplantation embryos: a role for oxidative stress in valproic acid-induced neural tube defects. Mol Pharmacol 80:979–87.

Ucciferri N, Collnot EM, Gaiser BK, Tirella A, Stone V, Domenici C, et al. 2014. *In vitro* toxicological screening of nanoparticles on primary human endothelial cells and the role of flow in modulating cell response. Nanotoxicology 8:697–708.

Verma A, Stellacci F. 2010. Effect of surface properties on nanoparticle–cell interactions. Small 6:12–21.

Wang Y, Chen L. 2011. Quantum dots, lighting up the research and development of nanomedicine. Nanomed Nanotech Biol Med 7:385–402.

Wick P, Malek A, Manser P, Meili D, Maeder-Althaus X, Diener L, et al. 2010. Barrier capacity of human placenta for nanosized materials. Environ Health Perspect 118:432–6.

Winnik FM, Maysinger D. 2012. Quantum dot cytotoxicity and ways to reduce it. Acc Chem Res 46:672–80.

Yang E, Korsmeyer SJ. 1996. Molecular thanatopsis: a discourse on the BCL2 family and cell death. Blood 88:386–401.

Yang H, Sun C, Fan Z, Tian X, Yan L, Du L, et al. 2012. Effects of gestational age and surface modification on materno-fetal transfer of nanoparticles in murine pregnancy. Sci Rep 2:847.

Yang RS, Chang LW, Wu JP, Tsai MH, Wang HJ, Kuo YC, et al. 2007. Persistent tissue kinetics and redistribution of nanoparticles, quantum dot 705, in mice: ICP-MS quantitative assessment. Environ Health Perspect 115:1339–43.

Yeh TK, Wu JP, Chang LW, Tsai MH, Chang WH, Tsai HT, et al. 2011. Comparative tissue distributions of cadmium chloride and cadmium-based quantum dot 705 in mice: safety implications and applications. Nanotoxicology 5:91–7.

Youle RJ, Strasser A. 2008. The BCL-2 protein family: opposing activities that mediate cell death. Nat Rev Mol Cell Biol 9:47–59.

Ziemba B, Janaszewska A, Ciepluch K, Krotewicz M, Fogel WA, Appelhans D, et al. 2011. *In vivo* toxicity of poly(propyleneimine) dendrimers. J Biomed Mater Res A 99:261–8.

Supplementary material available online

supplementary (Figure S1).